Performance Analysis for CNT-based SHM in Composite Structures

Seth S. Kessler, Gregory Thomas, Michael Borgen and Christopher T. Dunn

Metis Design Corporation

ABSTRACT

This paper presents results from a recent set of experiments devised to benchmark performance of a novel carbon nanotube (CNT) based approach for SHM in composite structures. CNT were bonded to cured carbon-fiber laminates using surfacing film, with electrodes embedded at either end. Five of each specimen was then subjected 3 types of damage: impact, cut slots and 4-point bending. For each type of test, resistance measurements were across the CNT network following each damage step, and during the 4-point-bending tests data was also collected under static load in addition to the unloaded state. Results indicate that the CNT networks exhibited little to no resistance change under nominal operating conditions, however significant resistance increases could be measured following events that permanently affected the composite laminates. CNT-based SHM has the potential to be a sensitive and reliable "witness" style damage detection method, while only introducing < 20 g/m^2 mass and < 100 µm in thickness.

INTRODUCTION

Carbon nanotubes (CNT) have the proven potential to increase the strength and stiffness of composite laminates (particularly interlaminar), but also can enable multifunctional structures through their increased electrical and thermal conductivity and their piezoresistive properties. Several morphologies of CNT enhancements have been investigated, ranging from radially-aligned CNT grown directly on host fibers throughout the laminate thickness (so-called "fuzzy fiber"), to vertically or horizontally-aligned electrically isolated CNT patches bonded in secondary processes (so-called "nanostiched"). From a design perspective, CNT are very beneficial in that the host plies can be designed for carrying structural loads while the CNT layer(s) can independently be optimized for other purposes such as embedded SHM, deicing and out of autoclave curing. This paper focuses on the analysis of performance for CNT-enhanced laminates for damage detection.

Seth S. Kessler, Metis Design Corporation, 205 Portland St, Boston, MA 02114, USA
Gregory Thomas, Metis Design Corporation, 205 Portland St, Boston, MA 02114, USA
Michael Borgen, Metis Design Corporation, 205 Portland St, Boston, MA 02114, USA
Christopher T. Dunn, Metis Design Corporation, 205 Portland St, Boston, MA 02114, USA

Initial testing to develop the CNT-based SHM method included impact detection (falling weight), delamination detection (following ASTM D5528-01) and detection of precursors to fracture (following ASTM D5776M-11). These tests were quite compelling, indicating repeatable response to extremely small damage levels in the CNT network in the form of a resistance change. Subsequently, in the present work the investigators set out to better quantify these resistance changes with respect to relatively controlled, but realistic, damage modes. The CNT specifically investigated herein were a multi-walled, axially aligned morphology. The individual nanotubes are ~100 um long and are manufactured using catalyzed, vapor deposition, such that the longitudinal axes of the nanotubes are all aligned. After manufacture, the CNT forests are densified to form a CNT "mat", such that the longitudinal axes of the nanotubes are still aligned, but now lie at a fixed angle with respect to the plane of the patch. This paper explores differential sheet resistivity of CNT networks in response to 3 specific loading conditions: impacting, slot-cutting, and 4-point-bending.

EXPERIMENTAL SETUP

CNT Specimens Preparation

A total of 15 woven graphite epoxy composite specimens were fabricated for testing, each measuring 300 x 25 x 3 mm. Both sides of the specimens were instrumented with an 80 x 25 mm centered forest of densified aligned carbon nanotubes (CNT) embedded within a Tencate surfacing film. Adhesive-mounted #4-40 x 6 mm threaded studs were installed at either end of each CNT forest to provide robust electrical contacts, and 50 μm thick expanded copper foil was placed over the top of the studs and pressed into ~ 6 mm at the edge of the CNT forest to provide a uniform current across the width of the specimens. The entire assembly was vacuum bagged and cured simultaneously at 130°C for 60 minutes. Spade-terminated wires were affixed to the studs post-cure, and all measurements were collected using a Fluke multimeter. An example of a pristine specimen can be seen in **Figure 1**, while examples of specimens after each type of destructive test can be seen in **Figure 2**.

Impact Testing

Guided dropped-mass impact tests were performed on 5 specimens, seen in **Figure 3**. Masses were mounted to a sleeve bearing carriage and guided by a vertical rail. The lower end of the rail was fixed to a baseplate that supported the specimen during impact. A 10 mm diameter steel rod bolted to the carriage served as the impact head, although the head did not directly contact the specimen during testing. A 10 x 40 mm steel bar was laid across the center of the specimen to absorb the direct impact and distributed the energy across the specimen width. A pocket was machined into the base plate that was slightly larger than the bar to leave the impact region unsupported, thus localizing the damage. Impact energies of roughly 5, 15, 30, 50, and 100 J were introduced. Mass was held constant at 7.25 kg while the carriage was lifted to the appropriate height to produce the desired impact energy.
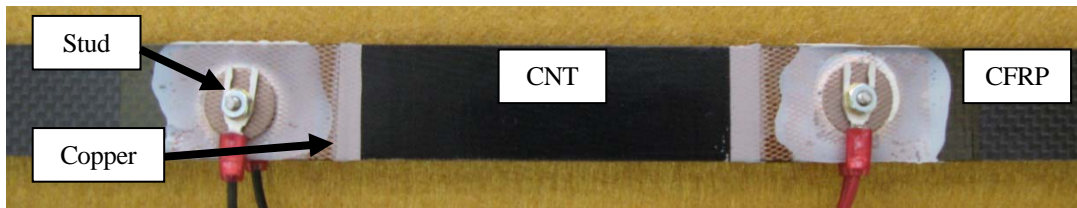
Figure 1: CFRP specimen with aligned CNT network embedded on front and back surface. Expanded copper mesh used to spread current to adhesively-mounted stud contacts.
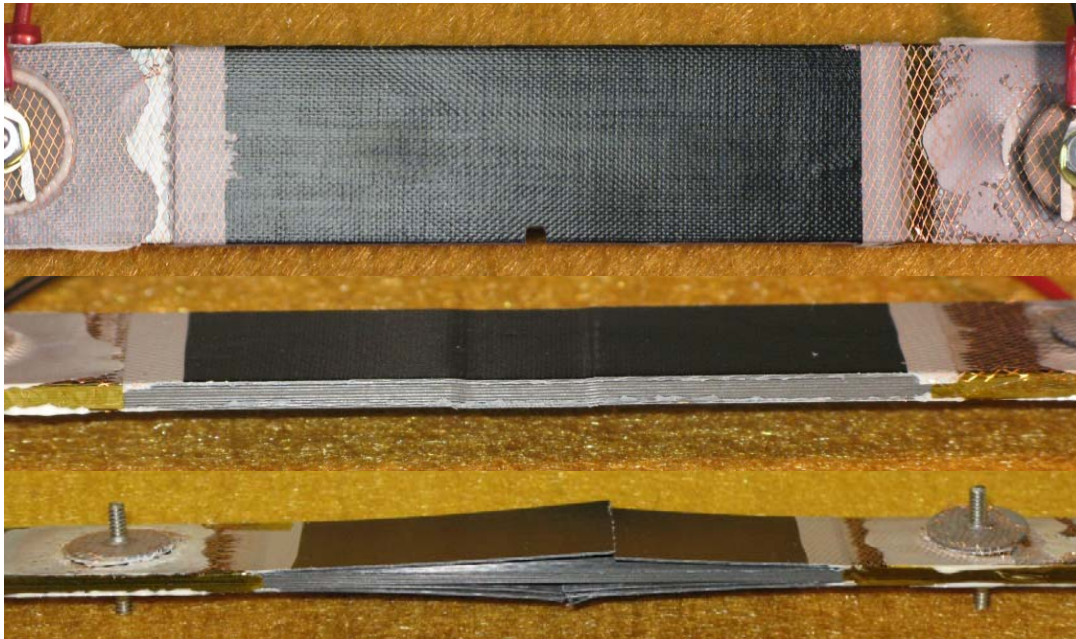

Figure 2: Examples of representative induced damage from testing; slot-cut (top), impact dislocation (middle) and ply tear accompanied by delmaination from 4-point bend overload (bottom)
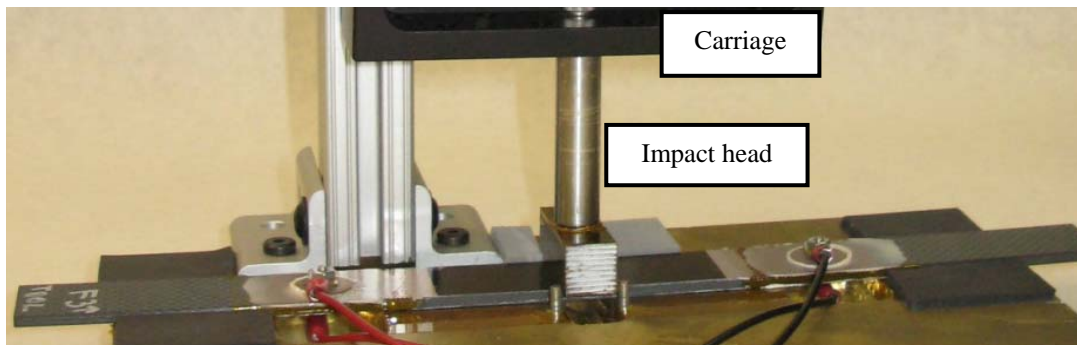

Figure 3: Example of impact test setup with steel bar between impact head and specimen
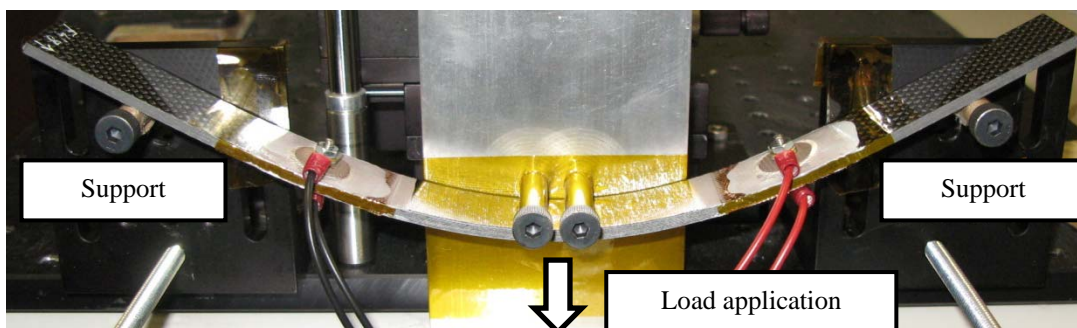

Figure 4: Example of loaded 4-point bend test specimen collected data while under ~ 300 N load

Slot-Cut Testing

To represent a fracture or tear in a laminate, slots were machined into 5 specimens. Three registration points on a clamp fixture were used to locate samples during cutting. The fixture itself referenced the fence of diamond wet-saw, enabling repeatable cuts through several cycles of removal and replacement. Nominal notch depths of 3, 6, 10, and 13 mm were cut into each specimen progressively with a 2.5 mm kerf blade.

4-Point-Bend Testing

To simulate damage caused by overload, a four-point bend fixture was constructed to provide a uniformly high stress between center rollers spaced by 13 mm, seen in **Figure 4**. Load application pins were guided by a ball bearing slide. Mass was applied to the slide carriage in 5 kg increments until 45 kg was reached, after which 2 kg increments were added until failure. Hysteresis was cleared between load steps by removing all load. CNT resistance was recorded under load and after load removal at each step. Displacement of the load carriage was measured at each step with a dial indicator accurate to ± 25 μm.

RESULTS

Impact Testing

The plotted raw data for the impact tests can be seen in **Figure 5**. While there is a large degree of variation in the data, as expected for this type of test, a number of meaningful trends can still be observed. Most importantly, the resistance was measured after each impact, illustrating that the change in resistance is permanent. For impacts with energy below a threshold value the change in resistance is negligible, while above the threshold energy the resistance increases rapidly. The threshold value for these specimens appears to be ~30 J, with < 0.25% change in resistance for all smaller impacts, after which the increase in resistance is broadly proportional to the amount by which the impact energy exceeds that threshold for a given specimen.

The strongest correlation in the data is for the impacted surface, which all exhibited ~1% change in resistance after 30 J impacts, and the majority of specimens showed an increase of ~15% after 110 J impacts. The majority of specimens also showed a larger increase in resistance for the CNT network installed on the opposite surface to impact (tensile side). Based on these results it could be said that any measured change in resistance > 1% definitively indicates real impact damage in these specimens. For a steady state resistance measurement it should be possible to reliably determine a 0.1% change in resistance, which means that it would be possible to increase the length of the CNT monitoring patch for these specimens to cover 1 m.

Slot-Cut Testing

The plotted raw data for the slot-cut tests can be seen in **Figure 6**. Also plotted is a simple numerical model that uses a 2D network of resistors arranged in a Cartesian array. The resistors are arranged on a 0.5 mm square grid, with the transverse and longitudinal resistor values chosen to match the measured CNT sheet resistivity. The measured data shows good agreement with the model, certainly within the limitations of the 0.5 mm grid resolution. It is important to note that the

model generally under-predicts the change in measured resistance. It is hypothesized that the divergence between the measured and simulated results is due to non-uniformity of the sheet resistivity in the CNT network from installation.

The simple numerical model shows that damage detection sensitivity is a strong function of the CNT network aspect ratio, defined as the ratio of the distance between the electrodes and the width of the network. For the 2400 mm² CNT area used for these tests (an aspect ratio of 3) a 160 mm² damaged area generates ~25% increase in total resistance. As the damage area grows, the resistance will increase in inverse proportion to the remaining current carrying width until the resistance becomes infinite when there is no electrical path. If the aspect ratio of the CNT network were to be increased to extend the monitoring area, the proportionate change in resistance with damage will decrease. For a 1 m long CNT network, a 160 mm² damage area would still produce a ~2% increase in the measured resistance, and even a 10 mm^2 slot would produce a change just over the noise floor.

4-Point-Bend Testing

The plotted raw resistance under load for the 4-point-bend tests can be seen in **Figure 7.** Also plotted is a simple numerical model predicting the response for the top and bottom CNT network resistances. The load/displacement curves for all specimens are in close agreement, indicating a high degree of repeatability. Using the initial slope of the load/displacement curve and a simple analytical model for the 4-point-bend stiffness, an Elastic Modulus can be calculated that is in good agreement with the expected value for this laminate. The data for CNT on either side of the specimen shows that the resistance change collected under load is broadly proportional to the strain while at low displacements. At larger displacements, when the specimen stiffness is no longer linear (and the laminate is likely permanently affected), the resistance change accelerates on the tensile side as resistance due to the CNT network being stretched-out is accumulated with the resistance increase due to network damage. Conversely, on the compressive side the resistance change decelerates as the net effect of the resistance decrease due to the CNT network being pushed together is tempered by resistance increase due to CNT network damage.

A more significant outcome of the 4-point-bend test can be seen in **Figure 8**, which plots the raw resistance change after unloading the specimen following each test increment. As these specimens exhibited the same permanence of resistance change due to damage as the prior types of tests, **Figure 8** essentially shows the same phenomenon observed in **Figure 7** with the reversible strain-induced response subtracted out. As seen in **Figure 8**, all specimens were in good agreement, and for loads < 300 N there was < 0.05% permanent change in resistance. However at larger loads and displacements, when the specimen stiffness is no longer linear (and the laminate is likely permanently affected) an exponential rise in resistance can be observed that is relatively consistent for all specimens, regardless of CNT network being in tension or compression. For this 4-point bend test, this resistance change is more indicative of precursors to damage than actual damage, thus the change magnitude is relatively small compared to the other tests conducted. While this measurement is still viably above the noise floor, the test area could not be expanded much past 10 cm without adding amplification in the test hardware, such as the type of circuits used for traditional foil strain gauges.
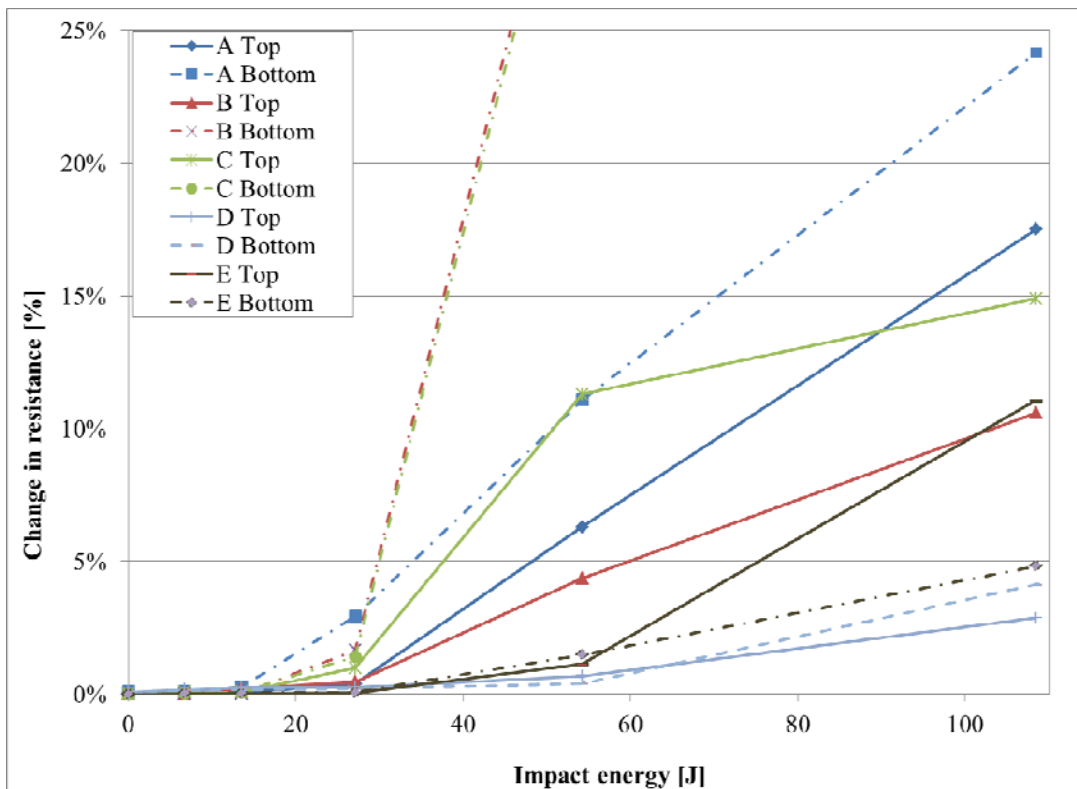
Figure 5: Impact test results for the CNT network. Less than 0.25% change obseved for impacts under 15 J, while significant changes are measured for impacts that introduced barely visible damage, up to 65% change for a 110 J impacts that creates a visible depression in the laminates.
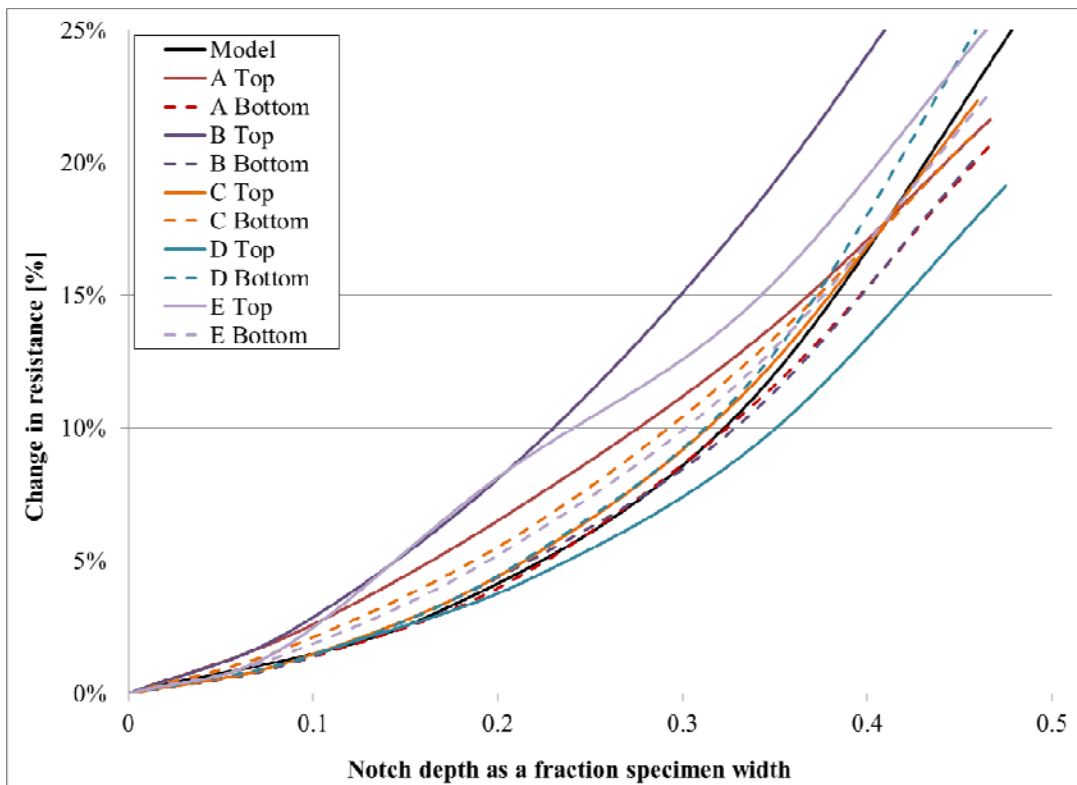

Figure 6: Slot-cut results for the CNT network, along with model prediction. CNT resistance grew steadily with slot extension, closely matching the model. Deviations caused by CNT network defects introduced in specimen integration as well as machining tolerances.
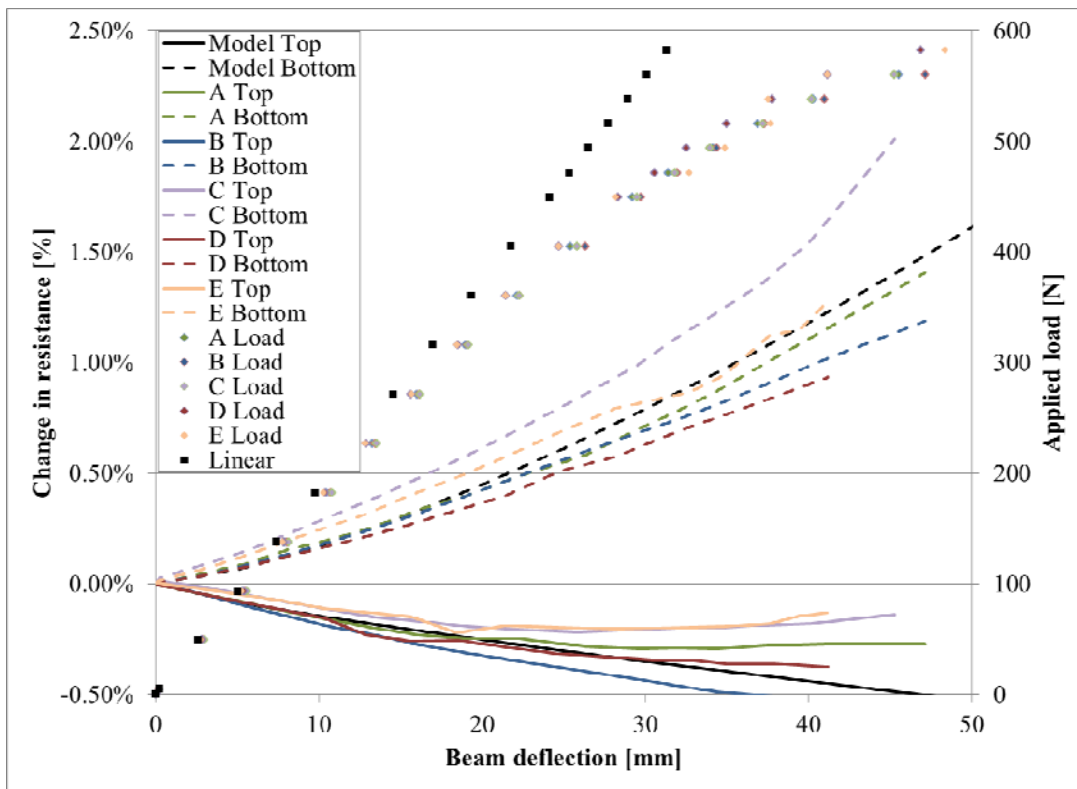
Figure 7: 4-point bend results for the CNT network collect under loading along with model predictions.
CNT network appears to track model well, particularly before load-curve becomes non-linear.
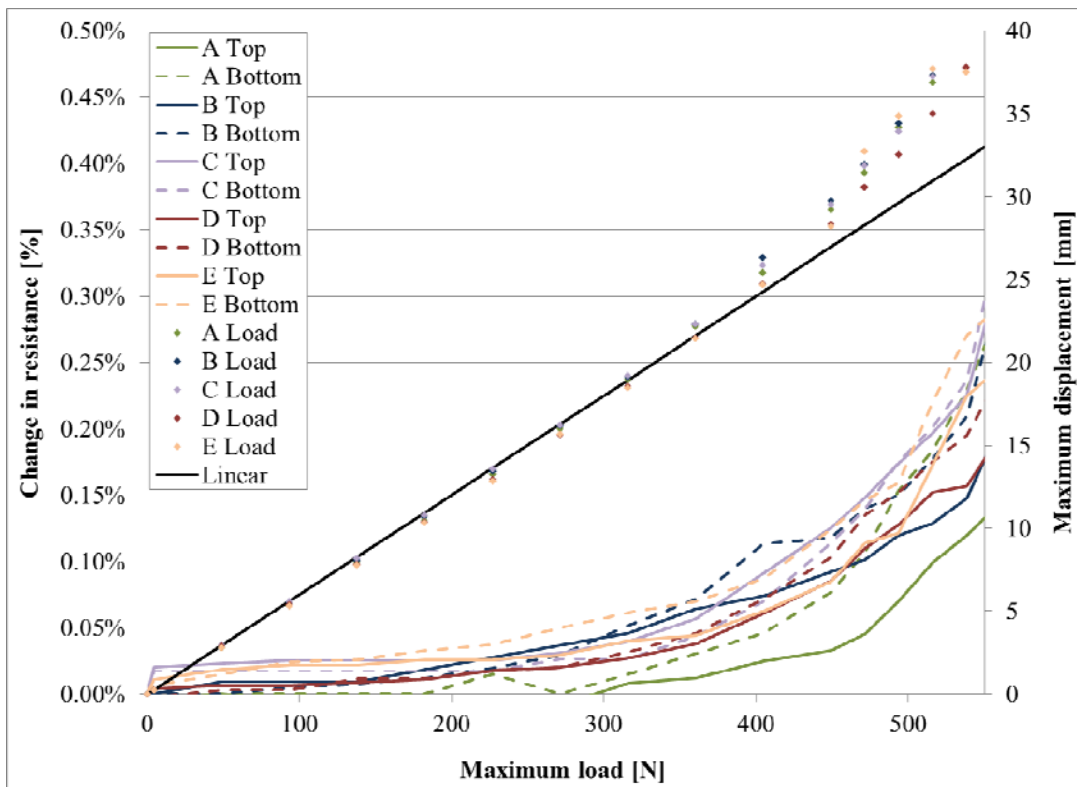Demonstrates ability of CNT network to be used as embedded strain gauge.

Figure 8: 4-point bend results for the CNT network collect without load. CNT network demonstrates
less than 0.05% change until load curve becomes non-linear, then changes accumulate with permanent
specimen deformation, appearently accelerating as damage becomes more severe before ultimate failure.

CONCLUDING REMARKS

This paper investigates the viability of using an aligned surface-mounted CNT network to detect damage in CFRP laminates. Three loading conditions were investigated: impact, slot-cuts and 4-point bending. The results clearly show that change in resistance of the CNT network directly correlates to the specimen loading exposure. Of particular interest, very little to no change is observed under static nominal conditions, but once irreversible damage is introduced into the specimens, permanent changes can be measured in the CNT network. Therefore the CNT sensor measurement does not have to be collected real-time, but could be collected post-operation as well. Being able to measure offline enables the use of many statistical methods to remove noise and operating environment effects, and will significantly improve the threshold and sensitivity of the measurement. In addition, because all 3 types of tests showed permanence, which implies that all of the measurements are additive and also integrate the loading history of the CNT network. Once calibrated for a specific application, this data could be used as part of a prognostic approach to provide remaining useful life (RUL) of a component.

ACKNOWLEDGMENTS

REFERENCES

1. Thostenson E.T., Ren Z. and Chou T.-W., "Advances in the science and technology of carbon nanotubes and their composites: a review," Composite Science and Technology, v. 61, pp. 1899-1912, 2001
2. Zhang W., Suhr J. and Koratkar N., "Carbon nanotube/polycarbonate composites as multifunctional strain sensors," Journal of Nanoscience and Nanotechnology, v. 6, pp. 960-4, 2006
3. Ajayan P.M. and Tour J.M., "Nanotube composites," Nature, v. 447, pp. 1066-8, 2007
4. Garcia, E.J., Wardle, B.L., and A.J. Hart, "Joining Prepreg Composite Interfaces with Aligned Carbon Nanotubes," *Composites Part A*, Vol. 39, 2008, pp. 1065-1070.
5. Veedu V.P., Cao A., Li X., Ma K, Solano C., Kar S. et al., "Multifunctional composites using reinforced laminae with carbon-nanotube forests," Nature Materials, v. 5, pp. 457-62, 2006
6. Beyakrova E., Thostenson E.T., Yu A., Kim H., Gao J., Tang J. et al., "Multiscale carbon nanotube-carbon fiber reinforcement for advanced epoxy composites," Langmuir, v. 23, pp. 3970-4, 2007
7. Du F.M., Fischer J.E., Winey K.I., "Effect of nanotube alignment on percolation conductivity in carbon nanotube/polymer composites," Physical Review B, v. 72(12), pp. 121404, 2004
8. Chou T.-W., Li C., and E.T. Thostenson. "Sensors and Actuators Based on Carbon Nantubes and Their Composites: A Review," Composites Science and Technology, 68(6) 1227-1249 (2008).
9. Wicks, S., Raghavan, A., Guzmán de Villoria, R., Kessler, S.S., and B.L. Wardle, "Tomographic Electrical Resistance-based Damage Sensing in Nano-Engineered Composite Structures," AIAA-2010-2871, *51st AIAA Structures, Structural Dynamics, and Materials (SDM) Conference*, Orlando, FL, April 12-15, 2010.
10. Garcia E.J., Wardle B.L., Hart J.A. and Yamamoto N., "Fabrication and multifunctional properties of a hybrid laminate with aligned carbon nanotubes grown in situ," Composite Science and Technology, v. 68, pp. 2034-41, 2008.
11. Wicks, S.S., Guzmán de Villoria, R., and B.L. Wardle, "Interlaminar and Intralaminar Reinforcement of Composite Laminates with Aligned Carbon Nanotubes," *Composites Science and Technology*, 70 (2010), pp. 20–28.
12. Guzmán de Villoria, R., Yamamoto, N., Miravete, A., and B.L. Wardle, "Multi-Physics Damage Sensing in Nano-Engineered Structural Materials," online in *Nanotechnology*, April 2011.